Improved Sensor Fusion for Flying Laptop Based on a Multiplicative EKF

Maximilian von Arnim[1], *Steffen Gaisser*[2], *Sabine Klinkner*[2]

Abstract
Flying Laptop is a small satellite carrying an optical communications payload. It was launched in 2017. To improve the satellite's attitude determination, which is used to point the payload, a new sensor fusion algorithm based on a low pass filter and a multiplicative extended Kalman filter (MEKF) was developed. As an operational satellite, improvements are only possible via software updates.

The algorithm estimates the satellite's attitude from star tracker and fibre-optical gyroscope (FOG) measurements. It also estimates the gyroscope bias. The global attitude estimate uses a quaternion representation, while the Kalman filter uses Gibbs Parameters to calculate small attitude errors. Past Kalman filter predictions are saved for several time steps so that a delayed star tracker measurement can be used to update the prediction at the time of measurement. The estimate at the current time is then calculated by predicting the system attitude based on the updated past estimate. The prediction step relies on the low-pass-filtered gyroscope measurements corrected by the bias estimate.

The new algorithm was developed as part of a master's thesis at the University of Stuttgart, where Flying Laptop was developed and built. It was simulated in a MATLAB/Simulink environment using the European Space Agency's GAFE framework. In addition, the new filter was applied to measurement data from the satellite. The results were used to compare the performance with the current filter implementation.

The new Kalman filter can deal with delayed, missing, or irregular star tracker measurements. It features a lower computational complexity than the previous standard extended Kalman filter used on Flying Laptop. The mean error of the attitude estimate was reduced by up to 90%. The low pass filter improves the rotation rate estimate between star tracker measurements, especially for biased and noisy gyroscopes. However, this comes at the cost of potentially less accurate attitude estimates. Educational satellites benefit from the new algorithm given their typically limited processing power and cheap commercial-off-the-shelf (COTS) sensors. This paper presents the approach in detail and shows its benefits.

Keywords
Attitude Determination Systems; Fibre-Optical Gyroscope; Kalman Filter; Sensor Fusion; Star Tracker

[1] Corresponding author: University of Stuttgart, Germany, maximilian.vonarnim@telematik-zentrum.de
[2] Institut für Raumfahrtsysteme, University of Stuttgart, Germany

Nomenclature

β	*Gyroscope bias*
ϑ	*Error angle*
ω	*Angular velocity*
A	*Assembly matrix*
F	*State matrix / jacobian*
H	*Observation matrix*
I	*Identity matrix*
P	*Filter covariance estimate*
q	*Quaternion*
Q	*Process noise covariance*
R	*Observation noise covariance*
t	*Time*
T	*Filter step time*
x	*System state*
$\otimes$	*(Shuster) quaternion multiplication*
$\hat{a}$	*Estimate of* a
$[a\times]$	*Cross product matrix of* a

Acronyms/Abbreviations

COI	*Center of Integration*
COTS	*Commercial-Off-The-Shelf*
EKF	*Extended Kalman Filter*
ESA	*European Space Agency*
FIR	*Finite Impulse Response*
FLOP	*Floating Point Operation*
FLP	*Flying Laptop*
FOG	*Fibre-Optical Gyroscope*
IIR	*Infinite Impulse Response*
LSQ	*Least Squares*
MEKF	*Multiplicative EKF*
MUKF	*Multiplicative UKF*
OLS	*Ordinary Least Squares*
PF	*Particle Filter*
STR	*Star Tracker*
UKF	*Unscented Kalman Filter*

1. Introduction

Flying Laptop (FLP) is a small satellite, developed and built at the University of Stuttgart. It measures $\mathbf{60}\times\mathbf{70}\times\mathbf{80}$ cm and has a mass of $\mathbf{110}$ kg [1]. A fixed optical communication system, OSIRISv1, is one of FLP's payloads. OSIRISv1 nominally requires an attitude determination accuracy of $\mathbf{0.034}$ mrad [2]. FLP carries two star trackers (STR A & B) and four fibre-optical gyroscopes (FOG) as high-precision attitude and rate sensors.

A standard extended Kalman filter (EKF) was previously developed for FLP. This filter was computationally expensive but did not achieve the required attitude determination performance [3], even after optimization [4].

Therefore, a new filter was sought. It was desired to reduce the risk of filter divergence, handle delayed, asynchronous and missing STR measurements, estimate the FOG bias and utilize oversampled FOG measurements.

FLP uses quaternions as attitude representation. This means that any algorithm must preserve the unit quaternion property [5]. The basic MEKF guarantees this by using a multiplicative error quaternion given in eq. (1) [5].

$$\boldsymbol{q^{true}} = \boldsymbol{\delta q}\otimes\boldsymbol{\hat{q}} \qquad (1)$$

Other popular filters such as unscented Kalman filters (UKF) [3, 6–11] or particle filters (PF) [12] exist but were dismissed as being too costly for the limited computational capacity of FLP [13]. They have their greatest strengths with highly nonlinear systems, whereas the rotation dynamics and kinematics can be linearized well for short time steps [5]. Recent UKF developments such as the Multiplicative UKF (MUKF) [14] are unproven and require adaptation to the sensors [13]. Conversely, combining low pass filtering with Kalman filters promises cheap noise reduction.

This paper presents a new filtering concept that combines low cost and high precision sensor fusion utilizing variable measurement rates.

2. Methodology

2.1. Definitions

This paper uses the same quaternion definition as [5] and the internal FLP algorithm, eq (2),

$$q = \begin{bmatrix} q_{1:3} \\ q_4 \end{bmatrix} = \begin{bmatrix} q_{x:z} \\ q_0 \end{bmatrix} \qquad (2)$$

for the quaternion product of $\boldsymbol{q}$ and $\boldsymbol{r}$ as eq. (3).

$$q\otimes r = \begin{bmatrix} q_4 I_3 - [q_{1:3}\times] & q_{1:3} \\ -q_{1:3}^T & q_4 \end{bmatrix} r \qquad (3)$$

It can be applied to vectors $\boldsymbol{\omega_{3\times1}}$ as shown in eq. (4) with the functions $\boldsymbol{\Omega,\Xi}$ given in [5].

$$\omega\otimes q = \begin{bmatrix} \omega \\ 0 \end{bmatrix}\otimes \mathrm{q} = \Omega(\omega)q = \Xi(q)\omega \qquad (4)$$

All reference frames are right-handed cartesian coordinate systems.

2.2. Filter Development

The new algorithm consists of three elements: A digital low pass filter to pre-process the raw gyroscope measurements, an ordinary least-squares (OLS) algorithm to fuse the gyroscope measurements in the satellite body frame, and finally a Kalman filter with a propagation and update step.

2.2.1. Low Pass Filtering Gyroscope Measurements

Five different 5th-order Cauer-type IIR filters were designed, one for each normalized cutoff

frequency $\omega_c \in \{\frac{1}{2}, \frac{1}{3}, \frac{1}{4}, \frac{1}{6}, \frac{1}{10}\}$, as they offer the lowest signal delay [8] [15]. The passband ripple was limited to $\delta_c = 0.002$ dB and the stopband attenuation was set to $\delta_s = -40$ dB to achieve minimal signal distortion and significant high-frequency noise suppression.

Least Squares for Gyroscope Fusion

A simple OLS algorithm was chosen to fuse the four partially redundant gyroscope measurements into a single three-dimensional measurement vector, utilizing the sensor assembly matrix A_{FOG} in eq. (5).

$$\omega_k^* = (A_{FOG}^T A_{FOG})^{-1} A_{FOG}^T \tilde{\omega}_k = A_{FOG}^* \tilde{\omega}_k \quad (5)$$

Modifying A_{FOG} allows an easy adaption to the case of missing gyroscope measurements.

2.2.2. Multiplicative Extended Kalman Filter

The new MEKF uses a propagation algorithm similar to [5]. It estimates a delta-state $\delta x_k = [\delta\vartheta_k, \beta_k]^T$ to determine the global state estimate q_k, ω_k. The rate measurement is adjusted with the bias estimate by eq. (6).

$$\hat{\omega}_k = \omega_k^* - \hat{\beta}_k \quad (6)$$

to propagate the attitude and covariance estimate. The discretization of the system Jacobian F_c (eq. (7)) is done via linearization in eq. (8) to minimize the computational effort [5].

$$F_c(t_{k-1}) = \begin{bmatrix} -[\hat{\omega}_{k-1}^+ \times] & I_3 \\ 0_{3\times3} & 0_{3\times3} \end{bmatrix} \quad (7)$$

$$F_{k-1} = I_6 + T_k F_c(t_{k-1}) \quad (8)$$

so that eqs. (9)- (11) propagate the state.

$$\hat{q}_k^- = exp\left(\frac{1}{2}\Omega(\hat{\omega}_{k-1}^+) T_k\right) \hat{q}_{k-1}^+ \quad (9)$$

$$\hat{\beta}_k^- = \hat{\beta}_k^+ \quad (10)$$

$$P_k^- = F_{k-1} P_{k-1}^+ F_{k-1}^T + Q \quad (11)$$

The à-priori estimate of the error angle is always set to zero (eq. (12)) as it is the best estimate given the data available for this step.

$$\delta\hat{\vartheta}_k^- = 0 \quad (12)$$

If no STR measurement was received, the filter execution ends here. The propagated value gets passed on to the controller and is added to the buffer for an eventual later update. If a STR measurement was received, the filter can proceed with the update step.

As the STR measurements can be taken asynchronously, their measurement must be compared with the estimated attitude $\hat{q}_{COI}^-$ at the time of measurement t_{COI}. This à-priori estimate is calculated by propagating from a previously buffered state using eq. (7) with an adjusted timestep $T_{COI} = t_{COI} - t_{k\ prior\ to\ COI}$. The error angle between a single STR measurement and estimate is given by eq (13).

$$\delta\vartheta_{STR} = 2\frac{(\mathrm{q}_\mathrm{r}^{-1} \otimes \mathrm{q}_\mathrm{STR} \otimes (\hat{\mathrm{q}}_\mathrm{COI}^-)^{-1})_{1:3}}{(\mathrm{q}_\mathrm{r}^{-1} \otimes \mathrm{q}_\mathrm{STR} \otimes (\hat{\mathrm{q}}_\mathrm{COI}^-)^{-1})_4} \quad (13)$$

If two STR measurements arrive in the same filter execution cycle, eq (13) is calculated for each measurement. The two error angles are then assembled by eq. (14).

$$\delta\vartheta_{STR\ AB} = \begin{bmatrix} \delta\vartheta_{STR\ A} \\ \delta\vartheta_{STR\ B} \end{bmatrix} \quad (14)$$

This gives the measurement Jacobian for a single measurement as eq. (15) and for two measurements as eq. (16).

$$H_A = H_B = [I_3 \quad 0_{3\times3}] \quad (15)$$

$$H_{AB} = \begin{bmatrix} H_A \\ H_B \end{bmatrix} \quad (16)$$

The matrices H and R for the Kalman gain must be chosen according to the number of STR measurements [13]. This leads to eq. (17) for the update of the error state.

$$\begin{bmatrix} \delta\hat{\vartheta}_k^+ \\ \hat{\beta}_k^+ \end{bmatrix} = \begin{bmatrix} \delta\hat{\vartheta}_k^- \\ \hat{\beta}_k^- \end{bmatrix} + K\delta\vartheta_{STR} \quad (17)$$

The global estimate prior to the COI is then updated with the error state per eqs. (1) and (6). The error quaternion is constructed from the error angle with eq. (18) using the definition of the Gibbs parameter [5].

$$\delta\hat{q}_k = \frac{1}{\sqrt{4 + \left(\delta\hat{\vartheta}_k^+\right)^T \delta\hat{\vartheta}_k^+}} \begin{bmatrix} \delta\hat{\vartheta}_k^+ \\ 2 \end{bmatrix} \quad (18)$$

With the oldest global state updated, the buffered FOG measurements can be used to propagate the updated state iteratively from the COI to the current time with eqs. (9)- (11). The propagated values replace the estimates in the buffer. If another STR measurement arrives in the next filter cycle, this updated buffer ensures that each update builds upon the best estimate at the time. An illustration of the algorithm is shown in Figure 8.

2.3. Simulations

The algorithm was simulated in MATLAB using ESA's GAFE framework [16] and the known parameters of FLP [13]. It is compared against the previous implementation. The true FOG bias and FOG noise are varied between simulation runs to determine the effect on the filter estimate. The initial values were chosen as

$$\hat{q}_0^+ = [0.5 \quad 0.5 \quad 0.5 \quad 0.5]^T \quad (19)$$

$$\hat{\omega}_0^+ = 0_{3\times1} \quad (20)$$

$$\delta\hat{x}_0^+ = \begin{bmatrix} \delta\hat{\vartheta}_0^+ \\ \hat{\beta}_0^+ \end{bmatrix} = 0_{6\times1} \quad (21)$$

$$P_0^+ = 1 \times 10^{-2}\, I_6 \quad (22)$$

2.3.1. Covariance Matrices

The measurement covariance matrix of each STR assumes uncorrelated noise, although a lower accuracy is expected for the around-boresight angle in eq. (23). Prior work with adaptive covariances was unsatisfactory [4].

$$R_A = R_B = diag([\sigma_{STR}^2 \quad \sigma_{STR}^2 \quad 10\sigma_{STR}^2]) \quad (23)$$

with $\sigma_{\mathrm{STR}}^2 = 10^{-11}$ [4]. The bias covariance is incorporated in the process noise covariance matrix. OLS is used to transform the four FOG variances into the bias estimate covariance [5].

$$Q = \begin{bmatrix} Q_\vartheta & 0 \\ 0 & A_{FOG}^* R_\beta (A_{FOG}^*)^T \end{bmatrix} \quad (24)$$

with eqs. (25) and (26) [4].

$$Q_\vartheta = diag([10^{-14} \quad 10^{-14} \quad 10^{-14}]) \quad (25)$$

$$R_\beta = diag([10^{-15} \quad 10^{-15} \quad 10^{-15}]) \quad (26)$$

3. Results and Discussion

3.1. Filter Estimation Performance

The new MEKF converges within 400s as shown in Figure 1 and Figure 2. Its attitude estimate error is unaffected by the FOG bias. Although the old EKF shows lower errors in the unbiased case in Figure 3, this advantage quickly vanishes when a bias is introduced in Figure 4. The new MEKF is more robust in this respect. While the desired accuracy is not reached yet, performance is improved.

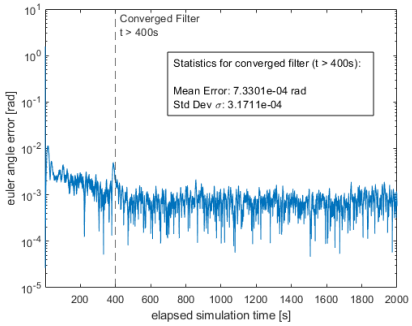

Figure 1: MEKF with unbiased FOG, Kalman filter at 5Hz, low pass filter $\omega_c = 0.25$

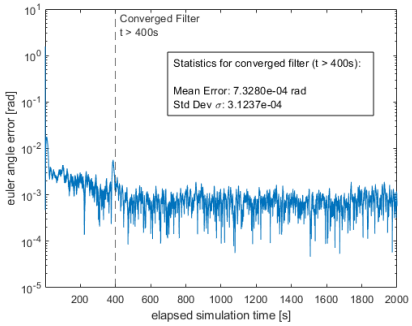

Figure 2: MEKF with FOG 0 bias $\beta = 10^{-2}\,\frac{rad}{s}$, Kalman filter at 5Hz, low pass filter $\omega_c = 0.25$

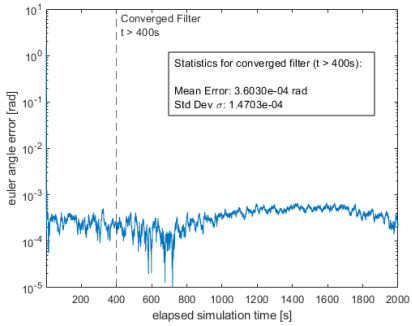

Figure 3: Old EKF with unbiased FOG, Kalman filter at 5Hz

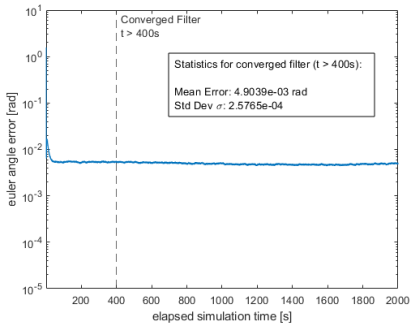

Figure 4: Old EKF with FOG 0 bias $\beta = 10^{-2}\,\frac{rad}{s}$, Kalman filter at 5Hz

The low pass filter is beneficial only if the Kalman filter cannot run fast enough to directly process all FOG measurements. The case where both the new MEKF and the FOGs run at 10Hz is shown in Figure 5 while the case with the MEKF running at 5Hz is given in Figure 6. Both the mean error, and the standard deviation of the mean, are improved in the latter case. Care must be taken to choose the correct cutoff frequency of the filter. A small cutoff frequency leads to signal delays that are too large for this relatively dynamic system. The optimum is found to lie around $0.2 < \omega_c < 0.5$.

3.2. Application to in-orbit data

The MEKF was applied FLP's in orbit measurements. This data included several periods without STR measurements, or only one STR providing data. This was due to blinding or high sensor noise preventing the STR's internal algorithm from finding a solution. The STRs are considered nearly exact for the purpose of analyzing the filter performance.

The result is shown in Figure 7 with two long periods without STR measurements, as well as brief gaps where a few samples are missing. The MEKF performs well.

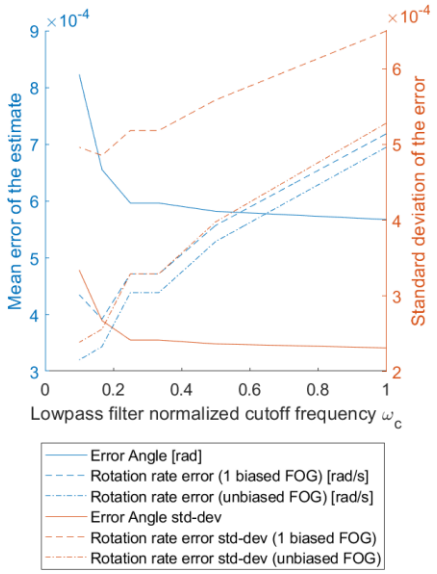

Figure 5: Error of the MEKF running at 10Hz depending on the cutoff frequency

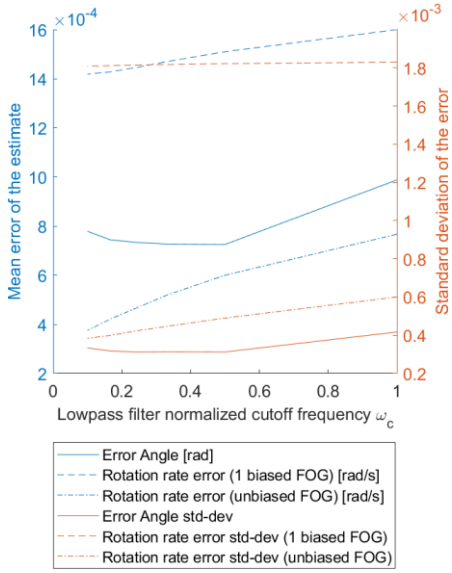

Figure 6: Error of the MEKF running at 5Hz depending on the cutoff frequency

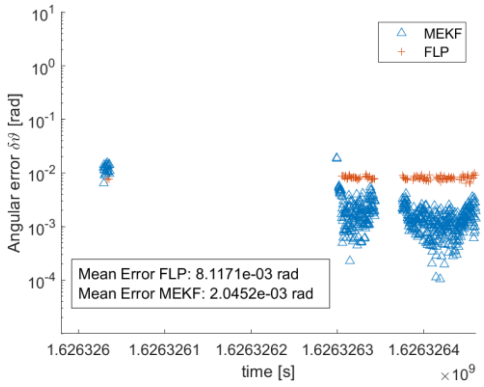

Figure 7: Error of the EKF running at 5Hz compared to the embedded FLP estimate using in-orbit STR and FOG data

3.3. Computational complexity

The required number of FLOPs was calculated theoretically [13]. The most expensive operations of the MEKF are the Kalman gain and the matrix exponential to propagate to the current. It is still more efficient than the old EKF, partially because the MEKF uses fewer measurement states. More iterations become necessary the longer the STR measurement is delayed. Both methods are equal for a STR delay of 2s, or 10 propagation steps [13].

4. Conclusions

A new sensor fusion algorithm was developed for FLP to try and improved its ACS based on a MEKF with a low pass filter to improve the filter robustness. Neither of the filters is quite able to reach the originally formulated required accuracy motivated by FLP's OSIRISv1 optical communications payload. However, the improved robustness should make communications more reliable. The new filter was shown to handle delayed and biased measurements in simulations, as well as missing measurements in real-world data from FLP. The low pass filter cutoff frequency needs to be optimized for the system and sensor parameters. Low pass filtering should only be combined with a Kalman filter if this enables the processing of additional measurements between two Kalman filter executions. The new MEKF it is advantageous in terms of FLOPs up to a STR measurement delay of 2s.

Acknowledgements

The first author would like to thank his co-authors for their support during the master thesis that laid the foundation for this paper.

References

[1] J. Eickhoff, The FLP Microsatellite Platform, Flight Operations Manual, 1st ed. 2016. Springer International Publishing, 2016.

[2] O. Zeile, Entwicklung einer Simulationsumgebung und robuster Algorithmen für das Lage- und Orbitkontrollsystem der Kleinsatelliten Flying Laptop und PERSEUS, Dissertation, Universität Stuttgart, 2012.

[3] P. Müller, Design and Implementation of Kalman Filters for the Attitude and Rate Estimation of a Small Satellite, IRS-11-S28, IRS-11-S28, Diplomarbeit, Universität Stuttgart, 2011.

[4] D. Triloff, Adaptation, Implementation and Verification of an Extended Kalman Filter for Sensor Fusion in the Attitude Control

System of the Small Satellite "Flying Laptop", IRS-17-S-083, IRS-17-S-083, Masterarbeit, Universität Stuttgart, 2017.

[5] F. L. Markley, J. L. Crassidis, Fundamentals of Spacecraft Attitude Determination and Control. Springer New York, 2014.

[6] J. Crassidis, F. L. Markley, Unscented Filtering for Spacecraft Attitude Estimation, *AIAA Guidance, Navigation and Control Conference and Exhibit*. Austin, Texas, 2003.

[7] K. Vinther, K. Fuglsang Jensen, J. A. Larsen, R. Wisniewski, Inexpensive CubeSat Attitude Estimation Using Quaternions and Unscented Kalman Filtering, *Automatic Control in Aerospace*, 4, 1, 1–12, 2011.

[8] E.-S. Park, S.-Y. Park, K.-M. Roh, K.-H. Choi, Satellite orbit determination using a batch filter based on the unscented transformation, *Aerospace Science and Technology*, 14, 6, 387–396, 2010.

[9] H. E. Soken, C. Hajiyev, Pico satellite attitude estimation via Robust Unscented Kalman Filter in the presence of measurement faults, *ISA transactions*, 49, 3, 249–256, 2010.

[10] P. Sekhavat, Q. Gong, I. M. Ross, NPSAT1 Parameter Estimation Using Unscented Kalman Filtering, *Proceedings of the 2007 American Control Conference*, 4445–4451, 2007.

[11] Y.-J. Cheon, J.-H. Kim, Unscented Filtering in a Unit Quaternion Space for Spacecraft Attitude Estimation, *2007 IEEE International Symposium on Industrial Electronics*, 66–71, 2007.

[12] Y. Cheng, J. Crassidis, Particle Filtering for Sequential Spacecraft Attitude Estimation, *AIAA Guidance, Navigation, and Control Conference and Exhibit*. Providence, Rhode Island, 2004.

[13] M. von Arnim, Design & Implementation of New Sensor Fusion Methods for Attitude Determination on the Small Satellite "Flying Laptop", IRS-21-S-020, Master's Thesis, Universität Stuttgart, 2021.

[14] K. Lee, E. N. Johnson, Robust Outlier-Adaptive Filtering for Vision-Aided Inertial Navigation, *Sensors (Basel, Switzerland)*, 20, 7, 2020.

[15] L. Wanhammar, T. Saramäki, Digital Filters Using MATLAB, 1st ed. 2020. Springer Nature Switzerland AG, 2020.

[16] D. Reggio, GAFE User's Manual, GAFE-UM-D7.5b, Issue 2.1, European Space Agency, 2019.

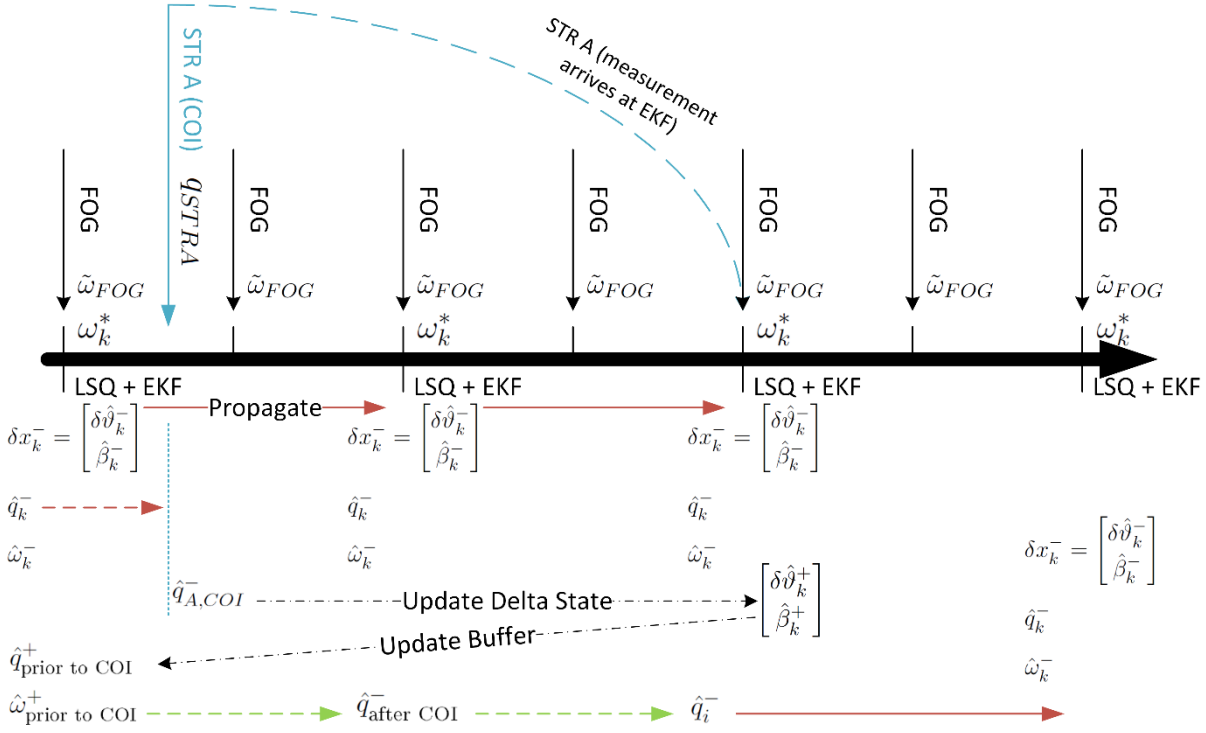

Figure 8: Schematic of the new algorithm with a single STR measurement